

Nuclear forces and neutron-rich systems

Achim Schwenk

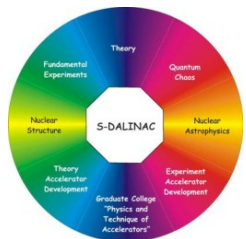


TECHNISCHE
UNIVERSITÄT
DARMSTADT



From few-nucleon forces to many-nucleon structure

ECT*, Trento, June 11, 2013



DFG



*Minerva
Stiftung*
ARCHES
Award for Research Cooperation and
High Excellence in Science



Bundesministerium
für Bildung
und Forschung

Outline

Chiral EFT and **many-body forces**

Neutron-rich nuclei and 3N forces

Neutron matter from chiral EFT interactions

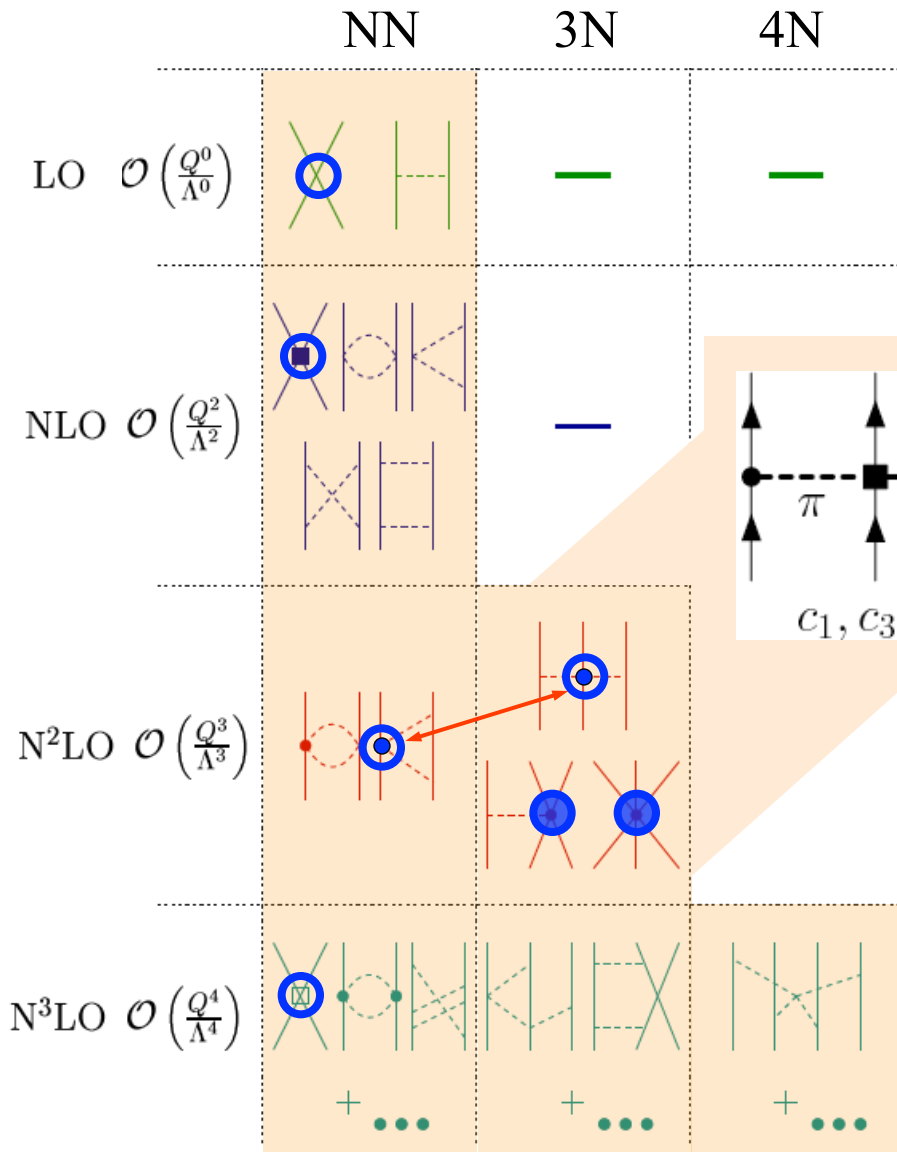
need for nonperturbative benchmark,
which parts of chiral EFT interactions are perturbative?

QMC calculations with chiral EFT interactions

Dark matter response of nuclei

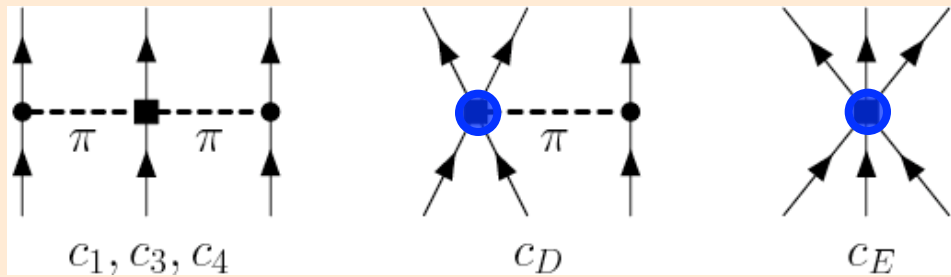
Chiral effective field theory and many-body forces

Separation of scales: low momenta $\frac{1}{\lambda} = Q \ll \Lambda_b$ breakdown scale ~ 500 MeV



consistent NN-3N-4N interactions

3N,4N: 2 new couplings to N³LO



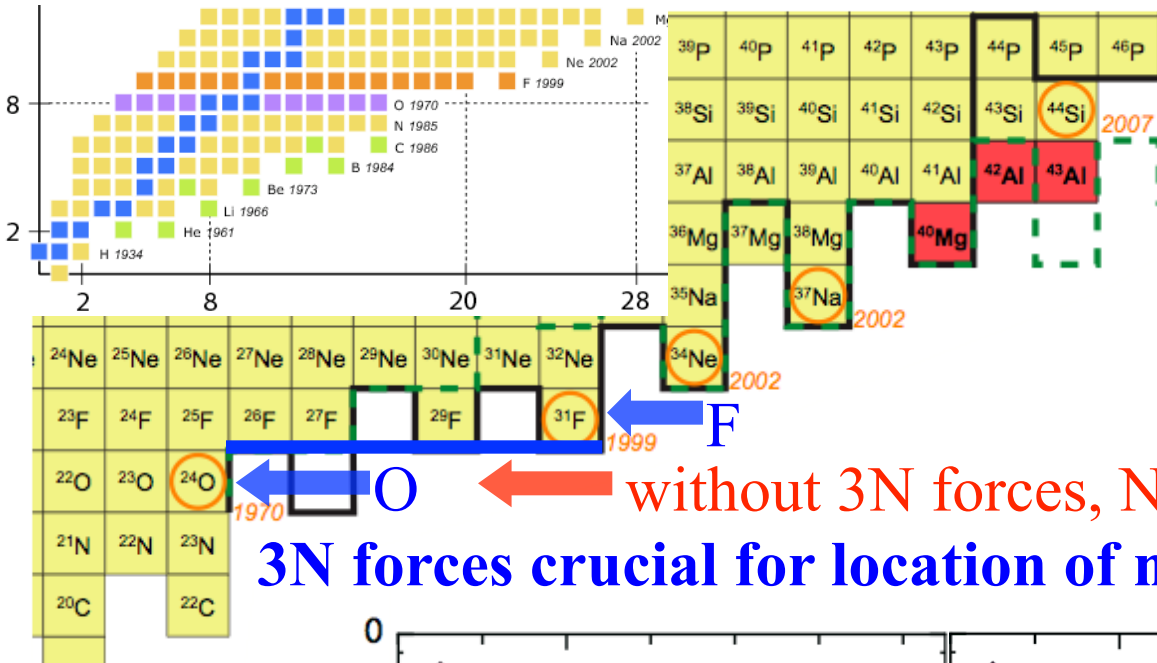
c_i from π N and NN [Meissner et al. \(2007\)](#)

$$c_1 = -0.9_{-0.5}^{+0.2}, \quad c_3 = -4.7_{-1.0}^{+1.2}, \quad c_4 = 3.5_{-0.2}^{+0.5}$$

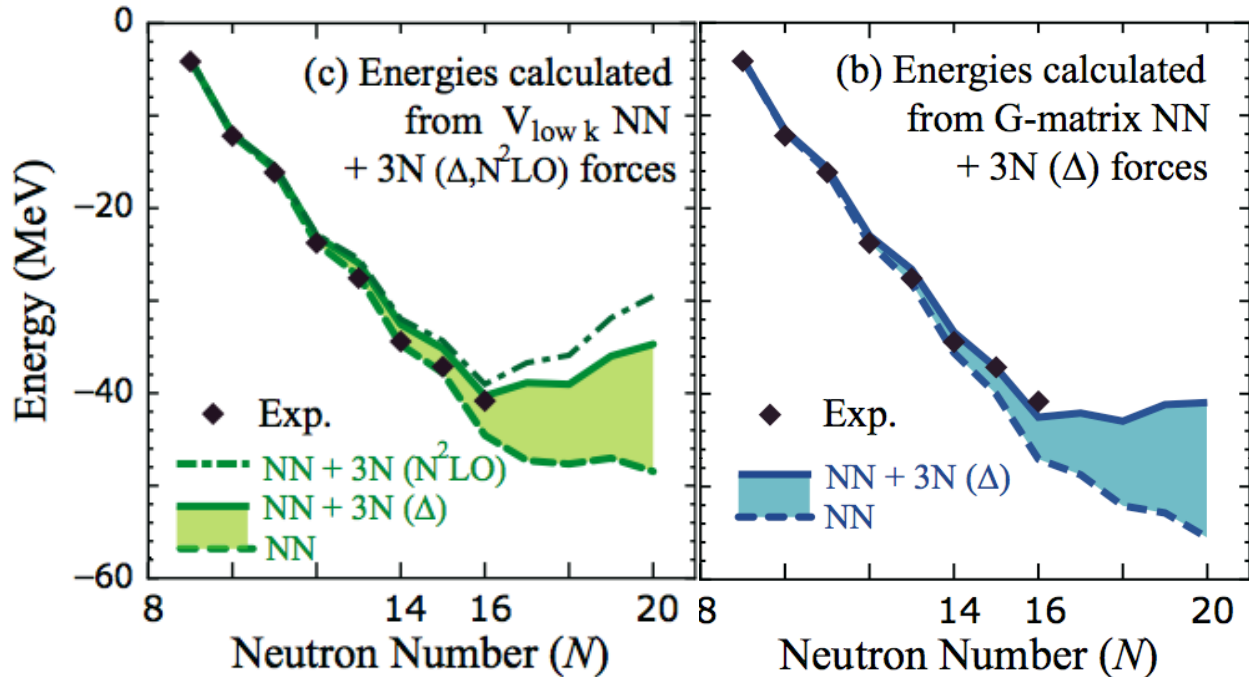
single- Δ : $c_1=0, c_3=-c_4/2=-3 \text{ GeV}^{-1}$

c_D, c_E fit to ${}^3\text{H}, {}^4\text{He}$ properties only

The oxygen anomaly Otsuka et al. (2010)



without 3N forces, NN interactions too attractive
3N forces crucial for location of neutron dripline



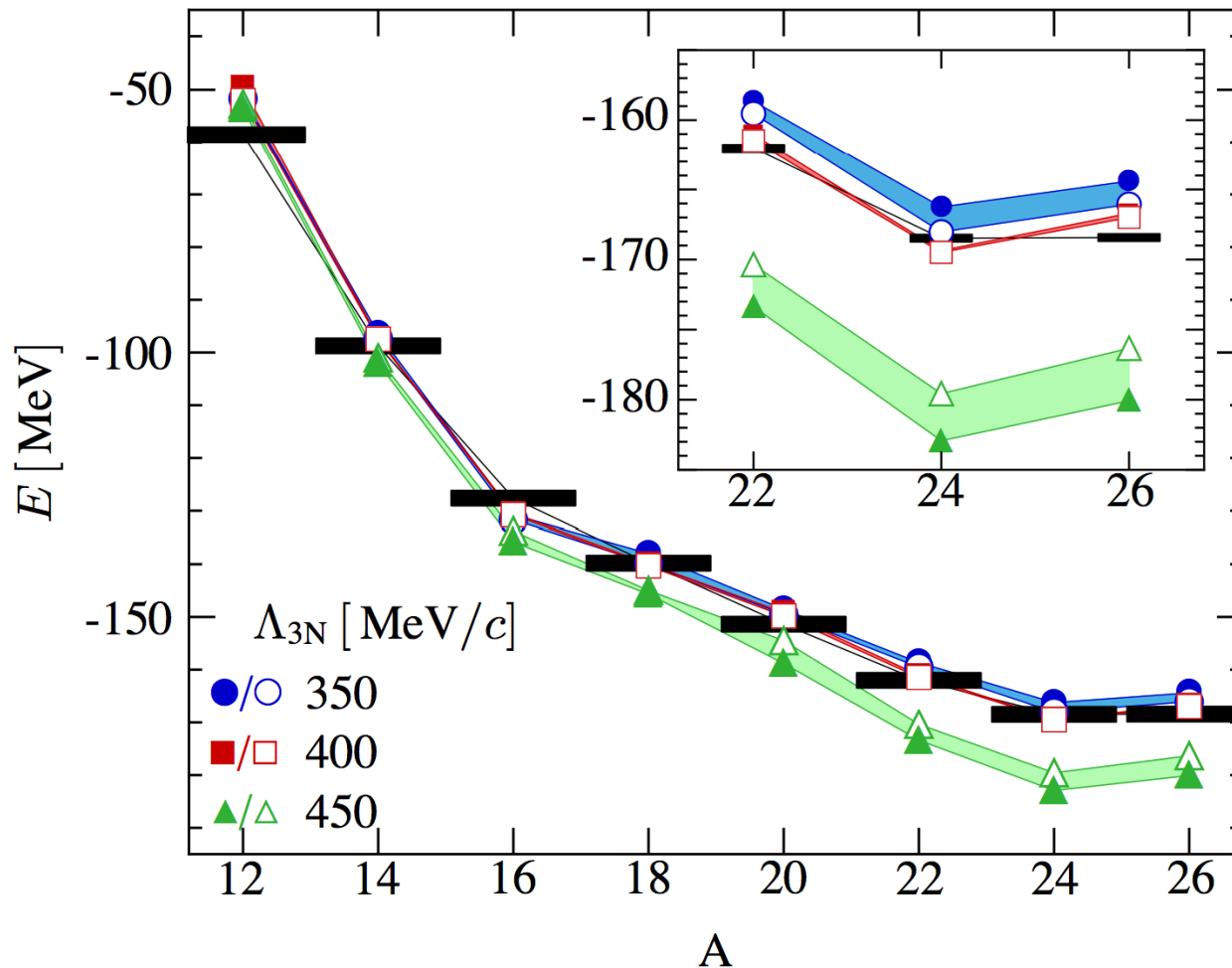
New ab-initio methods extend reach

impact of 3N forces confirmed in large-space calculations:

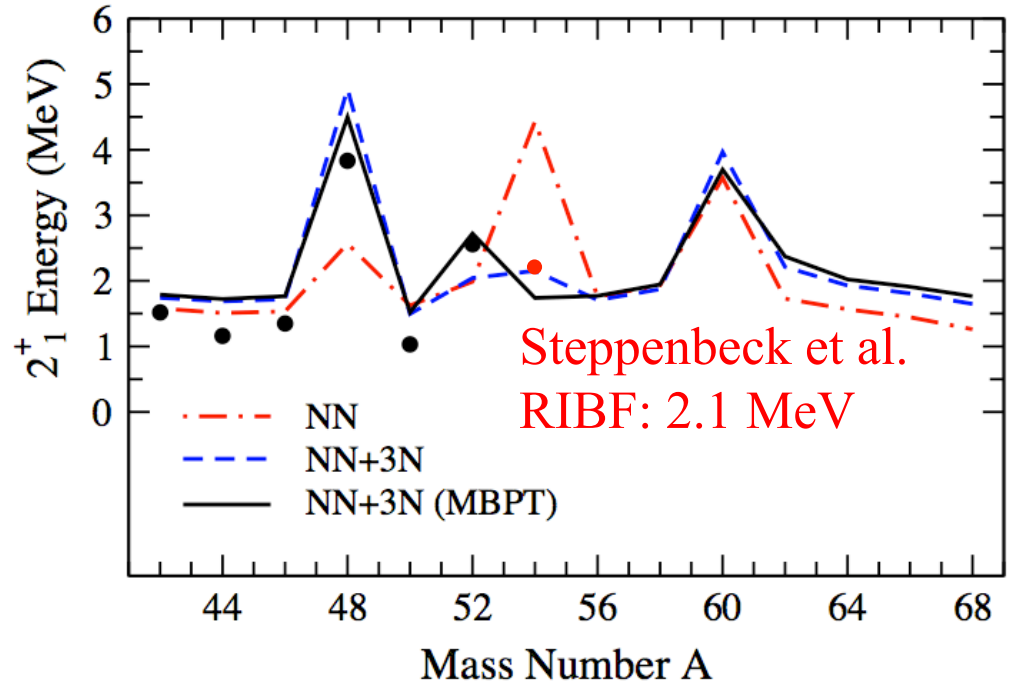
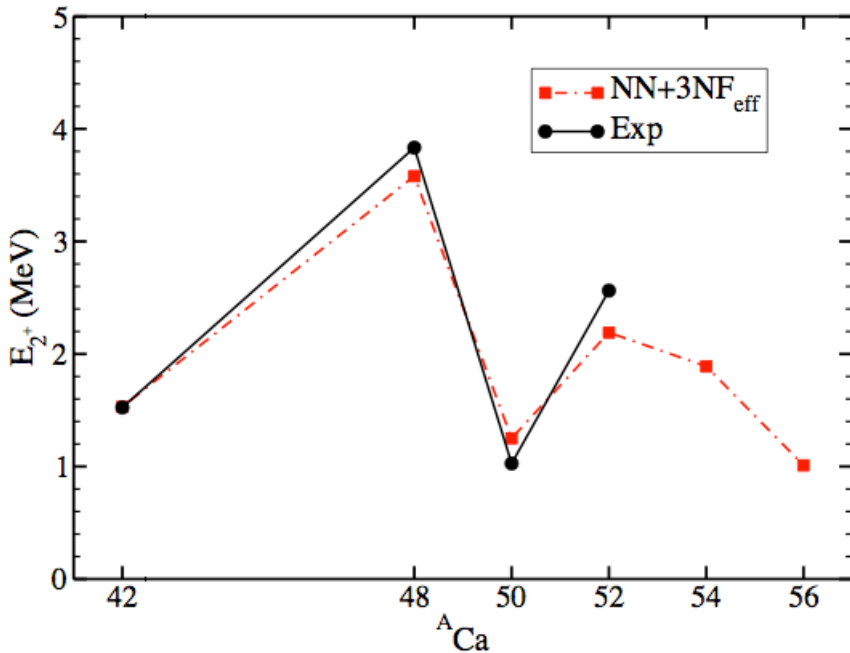
Coupled Cluster theory with phenomenological 3N forces [Hagen et al. \(2012\)](#)

In-Medium Similarity RG based on chiral NN+3N [Hergert et al. \(2013\)](#)

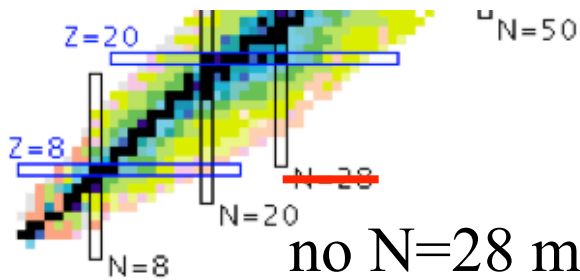
Green's function methods based on chiral NN+3N [Cipollone et al. \(2013\)](#)



Three-body forces and magic numbers



Hagen et al. (2012)



no N=28 magic number from microscopic NN forces

Zuker, Poves, ...

Holt et al. (2012, 2013)

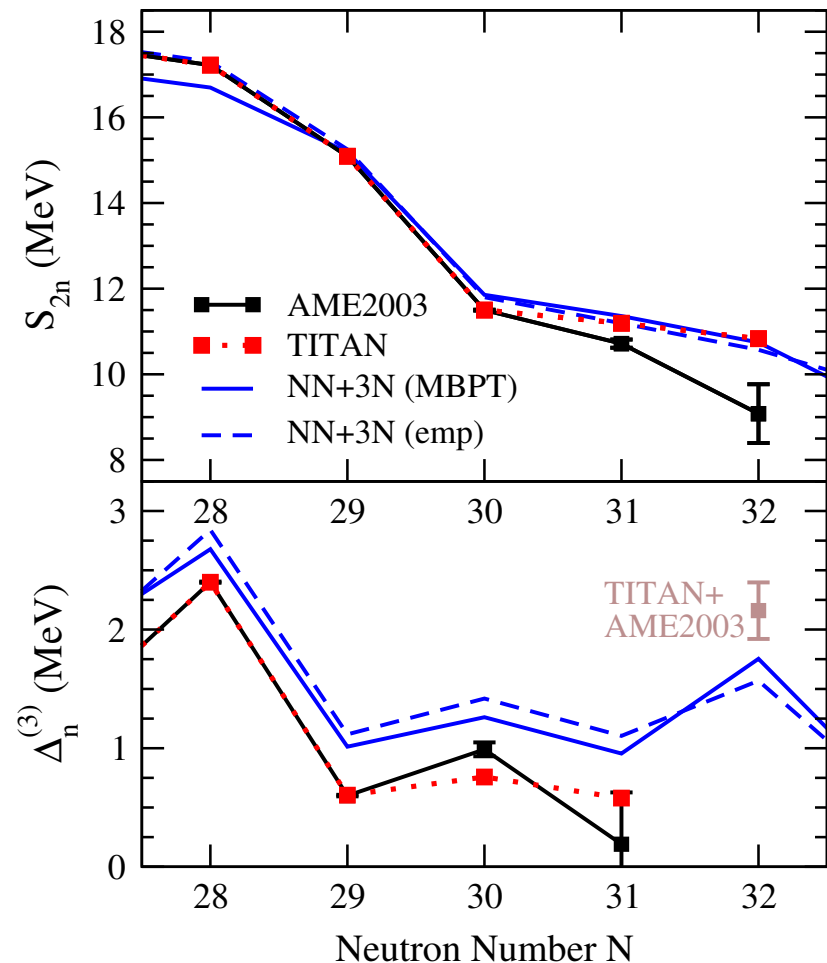
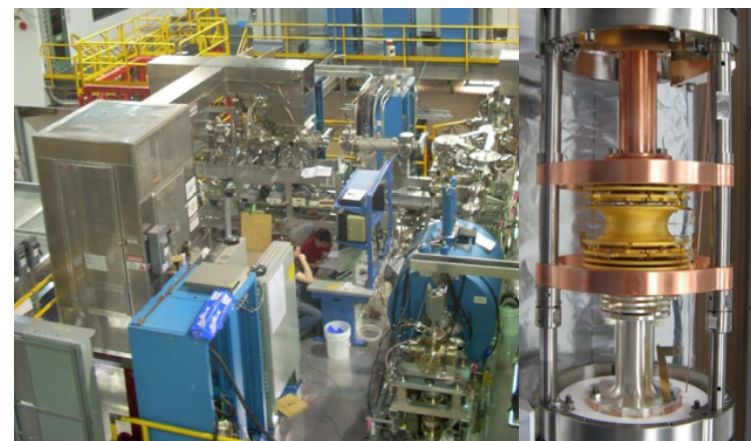
without 3N forces to 3rd order,
2⁺ is higher in ⁵⁴Ca

new $^{51,52}\text{Ca}$ TITAN measurements

^{52}Ca is 1.75 MeV more bound compared to atomic mass evaluation

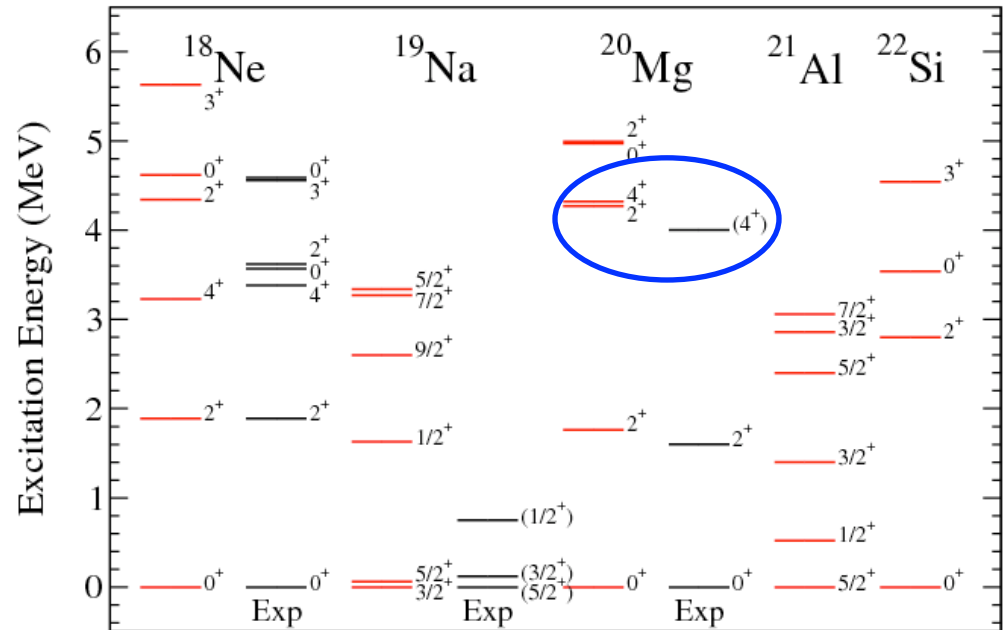
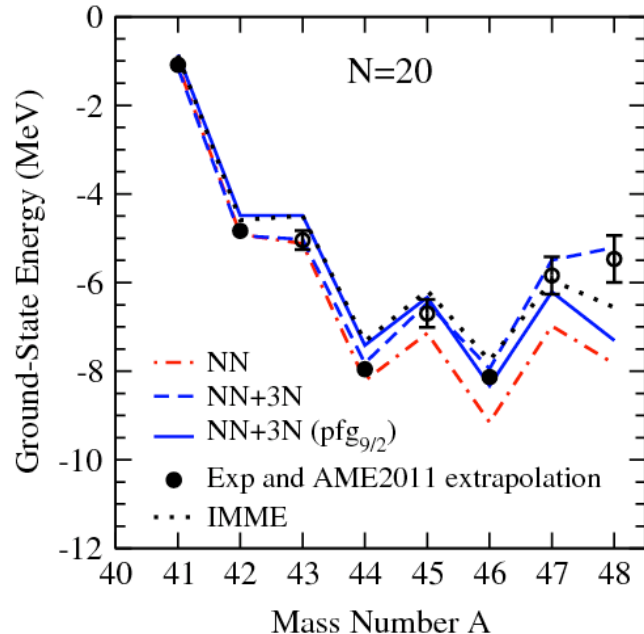
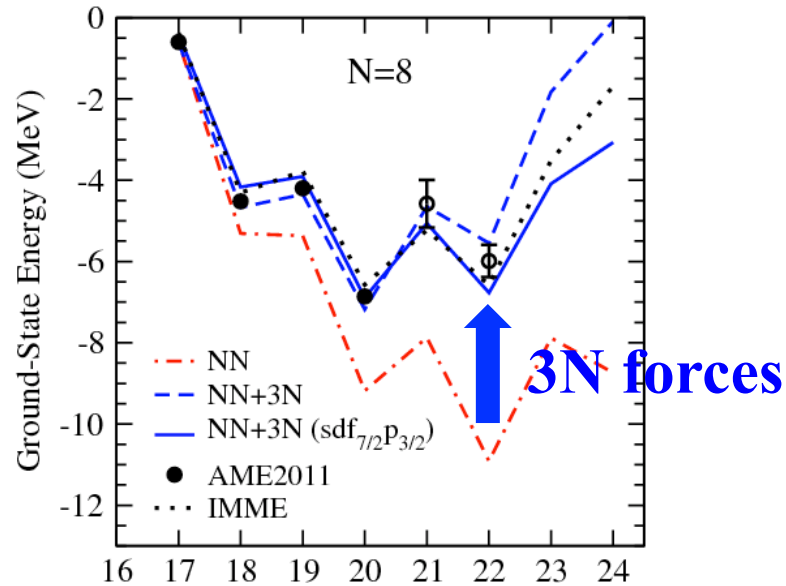
Gallant et al. (2012)

behavior of 2n separation energy S_{2n} agrees with NN+3N predictions



3N forces and proton-rich nuclei Holt, Menendez, AS (2013)

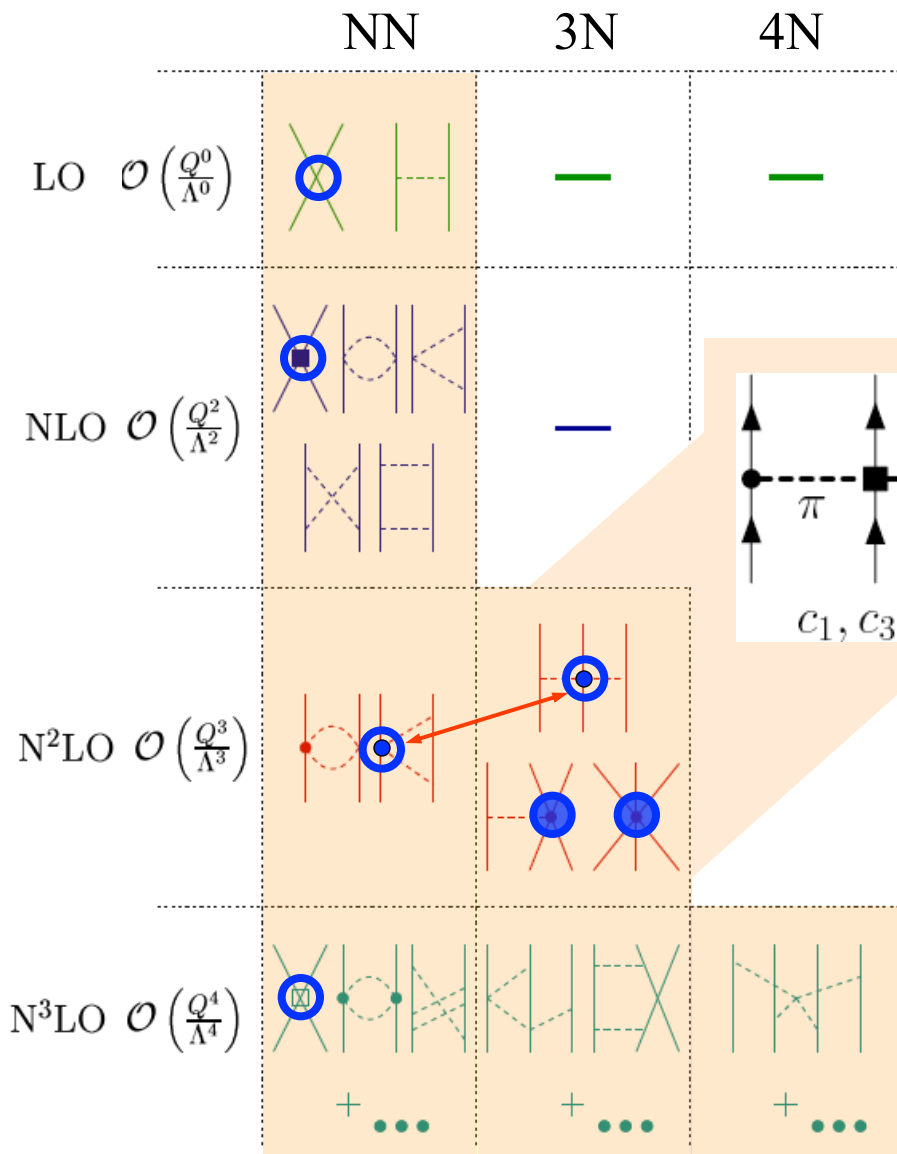
first results with 3N forces for ground and excited states of N=8, 20



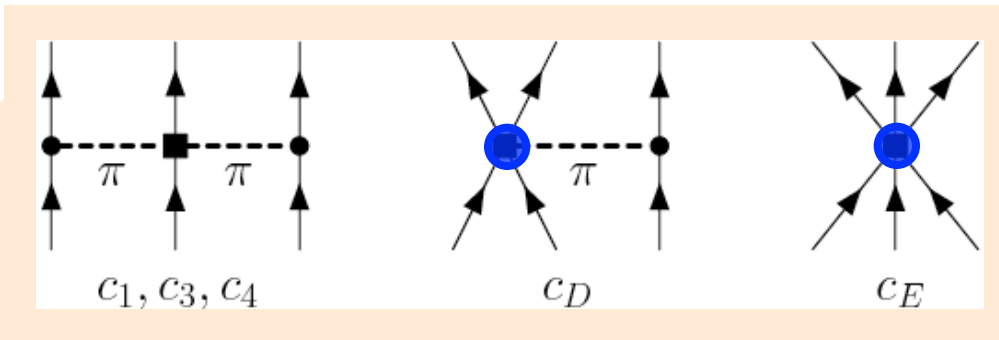
prediction for ²⁰Mg agrees with new state observed at GSI Mukha, private comm.

Chiral effective field theory for nuclear forces

Separation of scales: low momenta $\frac{1}{\lambda} = Q \ll \Lambda_b$ breakdown scale ~ 500 MeV



c_D, c_E don't contribute for **neutrons** because of Pauli principle and pion coupling to spin, also for c_4
 Hebeler, AS (2010)

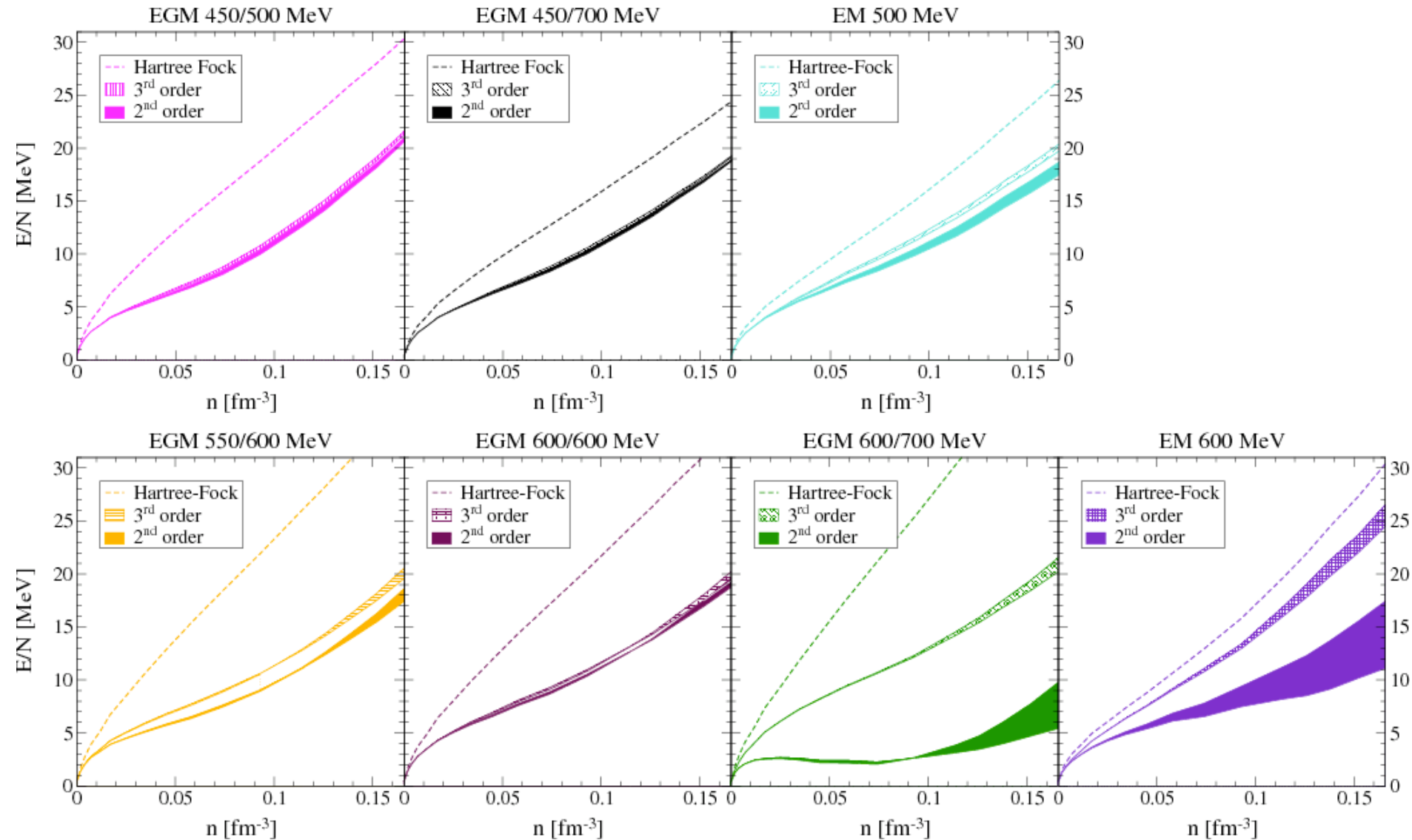


all 3- and 4-neutron forces are predicted to N³LO!

study 3N and 4N in neutron matter
 Tews, Krüger, Hebeler, AS (2013)

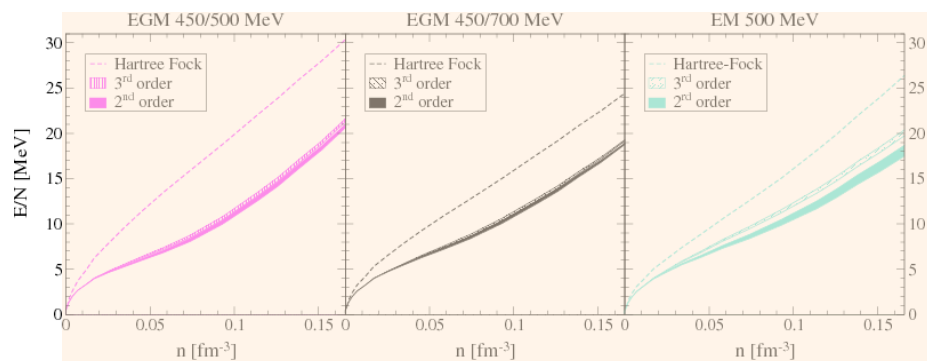
Neutron matter from chiral EFT interactions

direct calculations without RG/SRG evolution, 3N to N²LO only

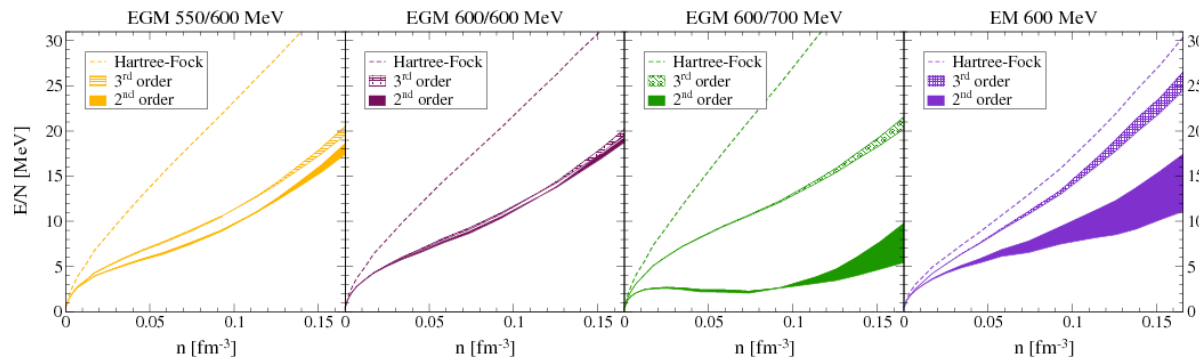


Measure of convergence and C_T values

N^3 LO NN potential	$ \Delta E_{\text{NN-only}}^{(2/3)} $	$ \Delta E_{\text{NN}/3N}^{(2/3)} $	$C_S [\text{fm}^2]$	$C_T [\text{fm}^2]$
EGM 450/500 MeV	0.8 MeV	0.6 MeV	-4.19	-0.45
EGM 450/700 MeV	0.4 MeV	0.4 MeV	-4.71	-0.24
EM 500 MeV	1.1 MeV	1.7 MeV	-3.90	0.22
EGM 550/600 MeV	1.0 MeV	3.1 MeV	-1.24	0.36
EGM 600/600 MeV	0.2 MeV	1.5 MeV	3.45	2.07
EGM 600/700 MeV	11.4 MeV	16.1 MeV	1.31	1.00
EM 600 MeV	7.7 MeV	9.1 MeV	-3.88	0.28

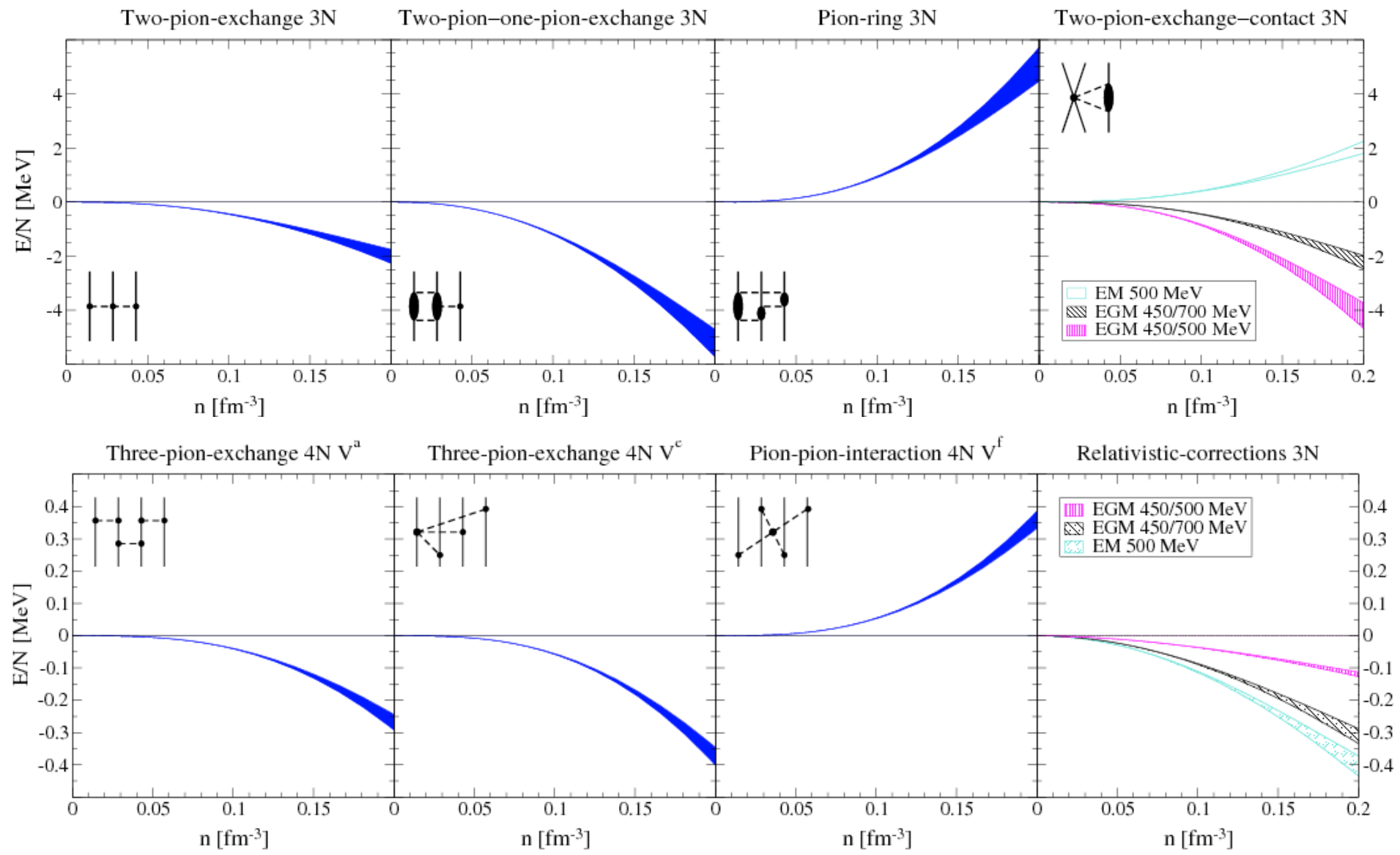


consider all NN interactions
with good convergence pattern
and small C_T



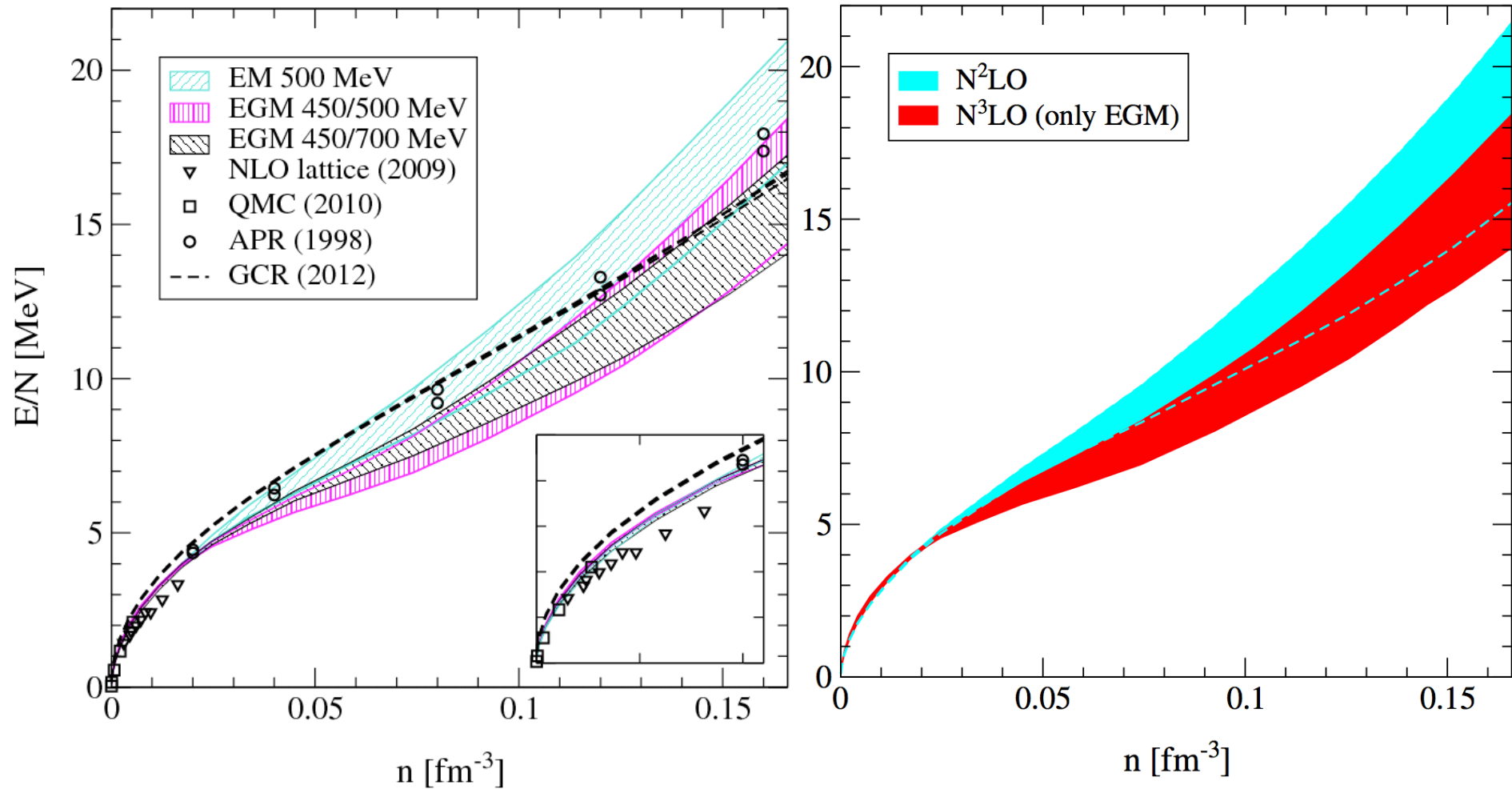
$N^3\text{LO}$ 3N and 4N interactions in neutron matter

evaluated at Hartree-Fock level

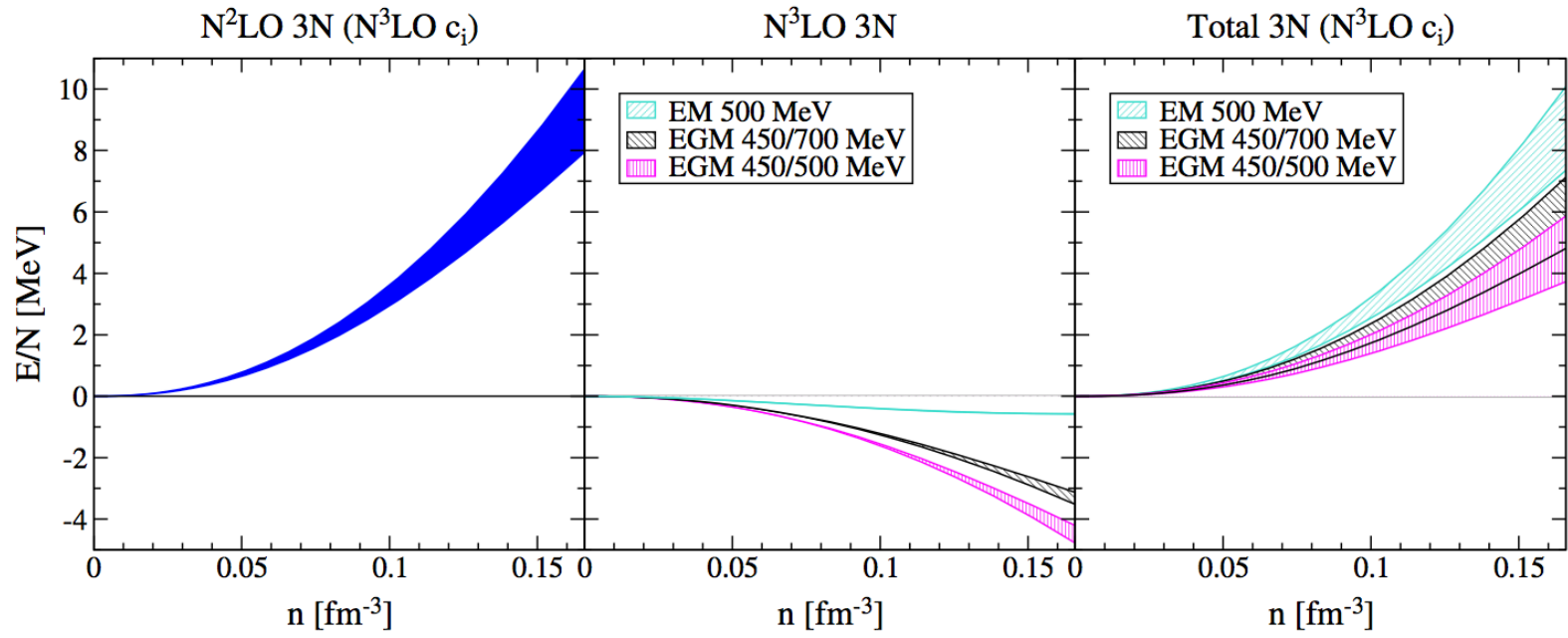


Complete N³LO calculation of neutron matter

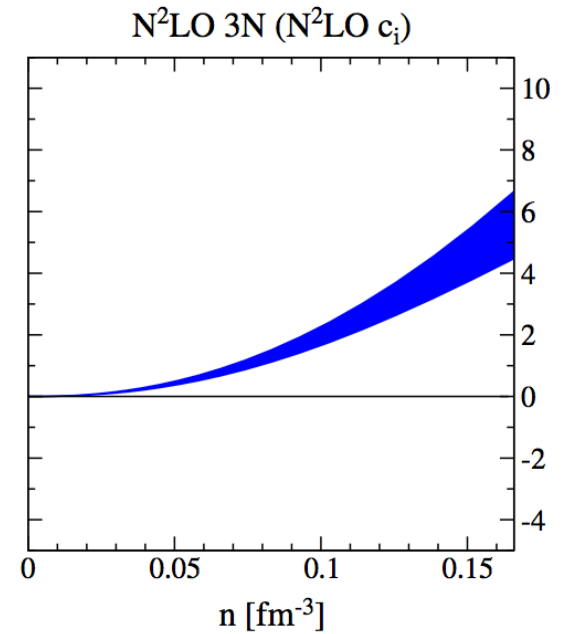
first complete N³LO result, Hartree-Fock +2nd order +3rd order (pp+hh)
includes uncertainties from NN, 3N (dominates), 4N



N²LO vs. N³LO 3N

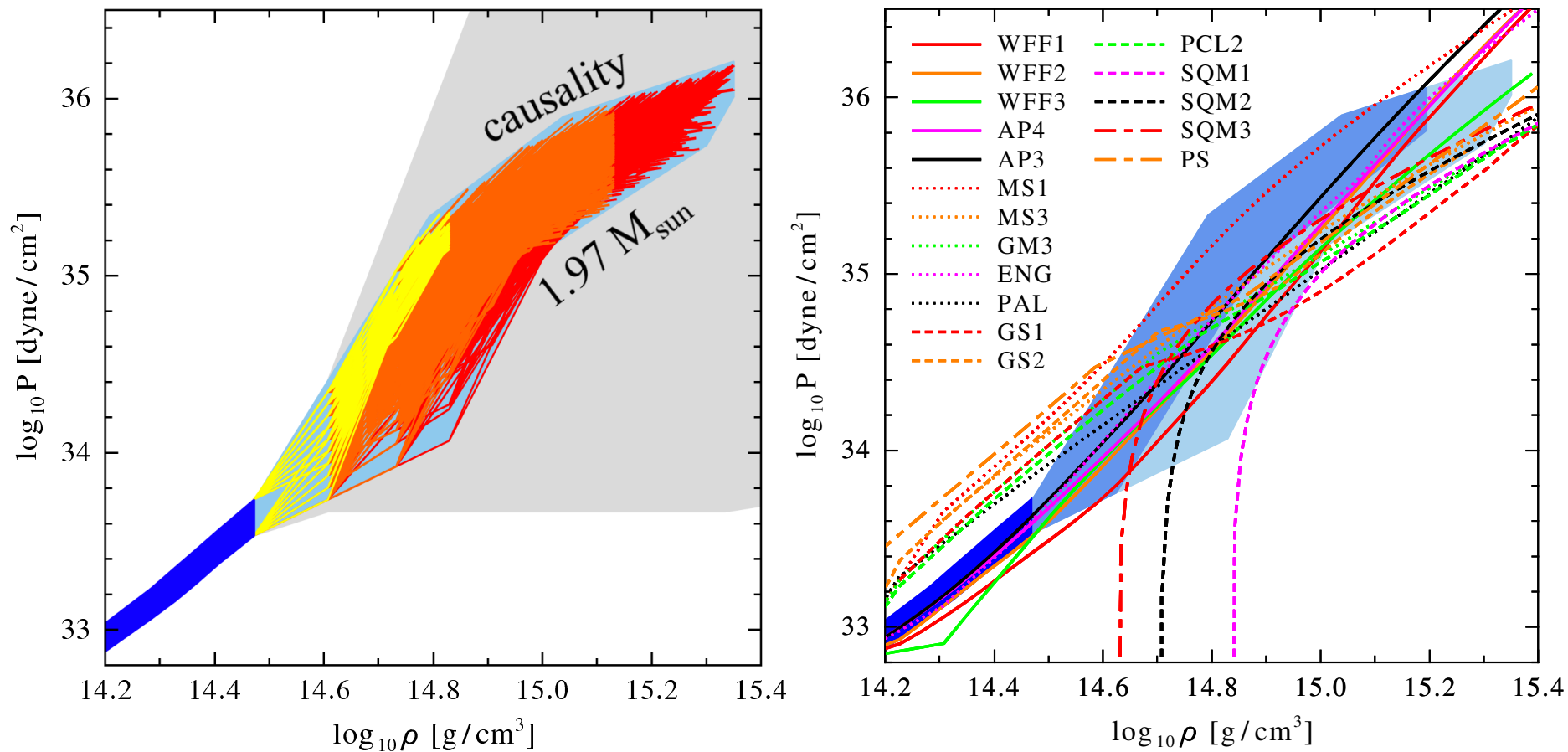


	c_1 [GeV ⁻¹]	c_3 [GeV ⁻¹]
N ² LO/N ³ LO EGM NN [31, 32]	-0.81	-3.40
N ³ LO EM NN [33, 34]	-0.81	-3.20
N ² LO KGE [39]	-(0.26 - 0.58)	-(2.80 - 3.14)
'N ² LO' KGE (recom.) [39]	-(0.37 - 0.73)	-(2.71 - 3.38)
N ³ LO KGE [39]	-(0.75 - 1.13)	-(4.77 - 5.51)
N ² LO this work	-(0.37 - 0.81)	-(2.71 - 3.40)
N ³ LO this work	-(0.75 - 1.13)	-(4.77 - 5.51)



Impact on neutron stars Hebeler, Lattimer, Pethick, AS (2010, 2013)

constrain high-density EOS by causality, require to support $1.97 M_{\text{sun}}$ star



low-density pressure sets scale, chiral EFT interactions provide strong constraints, ruling out many model equations of state

predicts neutron star radius: $9.7\text{-}13.9$ km for $M=1.4 M_{\text{sun}}$ ($\pm 18\%$!)

Neutron-star mergers and gravitational waves

explore sensitivity to neutron-rich matter in neutron-star merger and gw signal

Bauswein, Janka (2012), Bauswein, Janka, Hebeler, AS (2012).

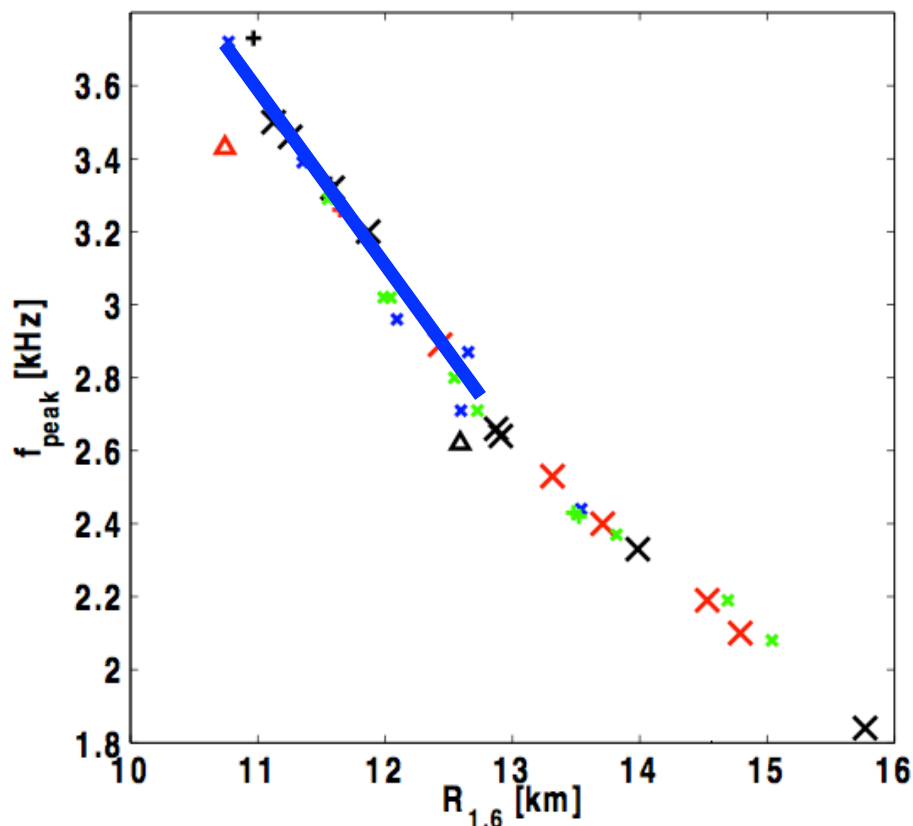


FIG. 10: Peak frequency of the postmerger GW emission versus the radius of a nonrotating NS with $1.6 M_{\odot}$ for different EoSs. Symbols have the same meaning as in Fig. 8.

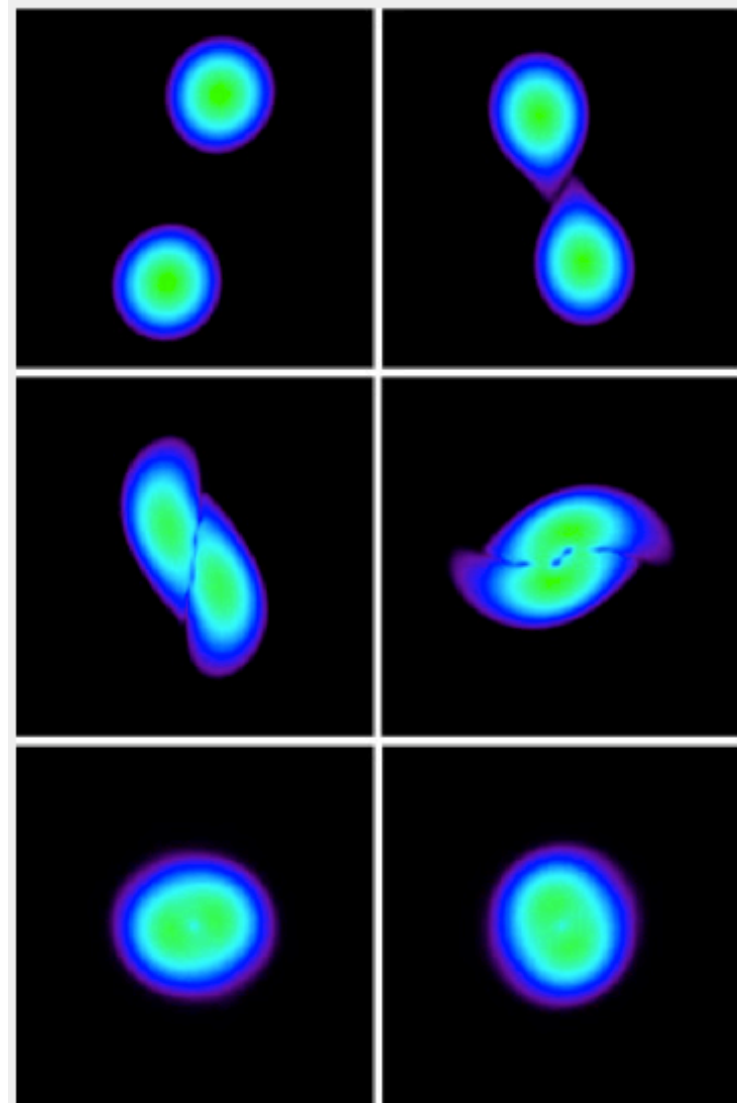


Fig. 1: Various snapshots of the collision of two neutron stars initially revolving around each other. The sequence simulated by the computer covers only 0.03 seconds. The two stars orbit each other counterclockwise (top left) and quickly come closer (top right). Finally they collide (centre left), merge (centre right), and form a dense, superheavy neutron star (bottom). Strong vibrations of the collision remnant are noticeable as deformations in east-west direction and in north-south direction (bottom panels). (Simulation: Andreas Bauswein and H.-Thomas Janka/MPA)

Symmetry energy and pressure of neutron matter

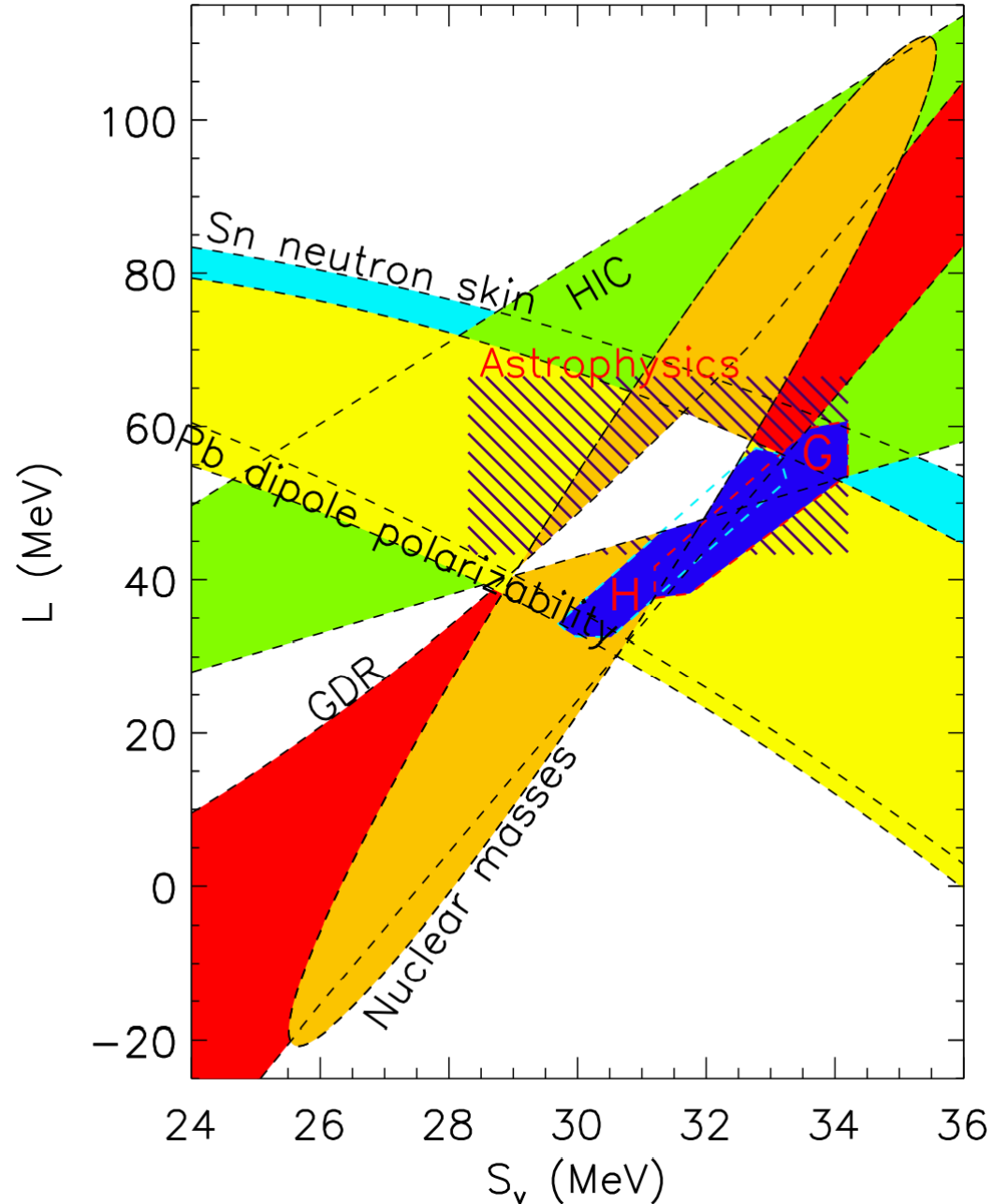
neutron matter band predicts
symmetry energy S_v and
its density derivative L

comparison to experimental
and observational constraints
Lattimer, Lim (2012)

neutron matter constraints
H: Hebeler et al. (2010) and in prep.

G: Gandolfi et al. (2011)

microscopic calculations
provide tight constraints!

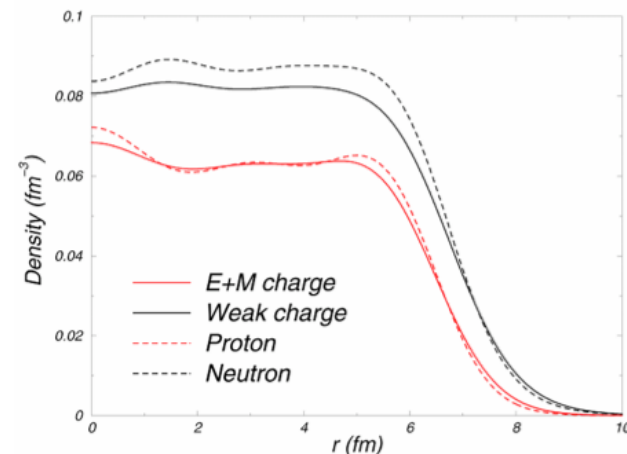


Neutron skin of ^{208}Pb

probes neutron matter energy/pressure,
neutron matter band predicts

neutron skin of ^{208}Pb : 0.17 ± 0.03 fm ($\pm 18\%$!)

Hebeler et al. (2010)



in excellent agreement with extraction from complete E1 response

$0.156 + 0.025 - 0.021$ fm

PRL 107, 062502 (2011)

PHYSICAL REVIEW LETTERS

week ending
5 AUGUST 2011

Complete Electric Dipole Response and the Neutron Skin in ^{208}Pb

A benchmark experiment on ^{208}Pb shows that polarized proton inelastic scattering at very forward angles including 0° is a powerful tool for high-resolution studies of electric dipole ($E1$) and spin magnetic dipole ($M1$) modes in nuclei over a broad excitation energy range to test up-to-date nuclear models. The extracted $E1$ polarizability leads to a neutron skin thickness $r_{\text{skin}} = 0.156^{+0.025}_{-0.021}$ fm in ^{208}Pb derived within

PREX: neutron skin from parity-violating electron-scattering at JLAB

electron exchanges Z-boson, couples preferentially to neutrons

goal II: ± 0.06 fm

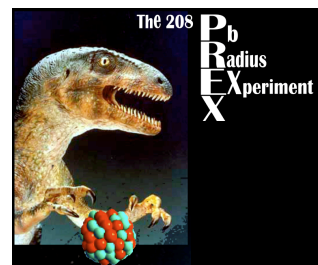
PRL 108, 112502 (2012)

PHYSICAL REVIEW LETTERS

week ending
16 MARCH 2012

Measurement of the Neutron Radius of ^{208}Pb through Parity Violation in Electron Scattering

We report the first measurement of the parity-violating asymmetry A_{PV} in the elastic scattering of polarized electrons from ^{208}Pb . A_{PV} is sensitive to the radius of the neutron distribution (R_n). The result $A_{\text{PV}} = 0.656 \pm 0.060(\text{stat}) \pm 0.014(\text{syst})$ ppm corresponds to a difference between the radii of the neutron and proton distributions $R_n - R_p = 0.33^{+0.16}_{-0.18}$ fm and provides the first electroweak observation of the neutron skin which is expected in a heavy, neutron-rich nucleus.



QMC with chiral EFT interactions - challenges

	NN	3N	4N
LO $\mathcal{O}\left(\frac{Q^0}{\Lambda^0}\right)$			
NLO $\mathcal{O}\left(\frac{Q^2}{\Lambda^2}\right)$			
N ² LO $\mathcal{O}\left(\frac{Q^3}{\Lambda^3}\right)$			
N ³ LO $\mathcal{O}\left(\frac{Q^4}{\Lambda^4}\right)$			

EFT includes nonlocal interactions

caused by usual regulator
on relative momenta

and k-dependent contact interactions
k=mom. transfer in exchange channel

pion exchanges to N²LO local
except for regulator

strategies so far:
try directly in QMC

Lynn, Schmidt

separate local + nonlocal parts
and treat nonlocal perturbatively

Furnstahl, Wendt

Local chiral EFT interactions

keep pion exchanges to N²LO local

regulate in coordinate space $f_{\text{long}}(r) = 1 - e^{-(r/R_0)^4}$

construct local contact interactions $C_S + C_T \boldsymbol{\sigma}_1 \cdot \boldsymbol{\sigma}_2$

with regulator on momentum transfer $\int \frac{d\mathbf{q}}{(2\pi)^3} C_{S,T} f_{\text{local}}(q^2) e^{i\mathbf{q}\cdot\mathbf{r}} = C_{S,T} \frac{e^{-(r/R_0)^4}}{\pi\Gamma(\frac{3}{4})R_0^3}$

at NLO use freedom to treat k^2 operators for isospin dependence

$$\begin{aligned}
 V_{\text{short}}^{\text{NLO}} = & C_1 q^2 + C_2 q^2 \boldsymbol{\tau}_1 \cdot \boldsymbol{\tau}_2 \\
 & + (C_3 q^2 + C_4 q^2 \boldsymbol{\tau}_1 \cdot \boldsymbol{\tau}_2) \boldsymbol{\sigma}_1 \cdot \boldsymbol{\sigma}_2 \\
 & + i \frac{C_5}{2} (\boldsymbol{\sigma}_1 + \boldsymbol{\sigma}_2) \cdot \mathbf{q} \times \mathbf{k} \\
 & + C_6 (\boldsymbol{\sigma}_1 \cdot \mathbf{q})(\boldsymbol{\sigma}_2 \cdot \mathbf{q}) \\
 & + C_7 (\boldsymbol{\sigma}_1 \cdot \mathbf{q})(\boldsymbol{\sigma}_2 \cdot \mathbf{q}) \boldsymbol{\tau}_1 \cdot \boldsymbol{\tau}_2,
 \end{aligned}$$

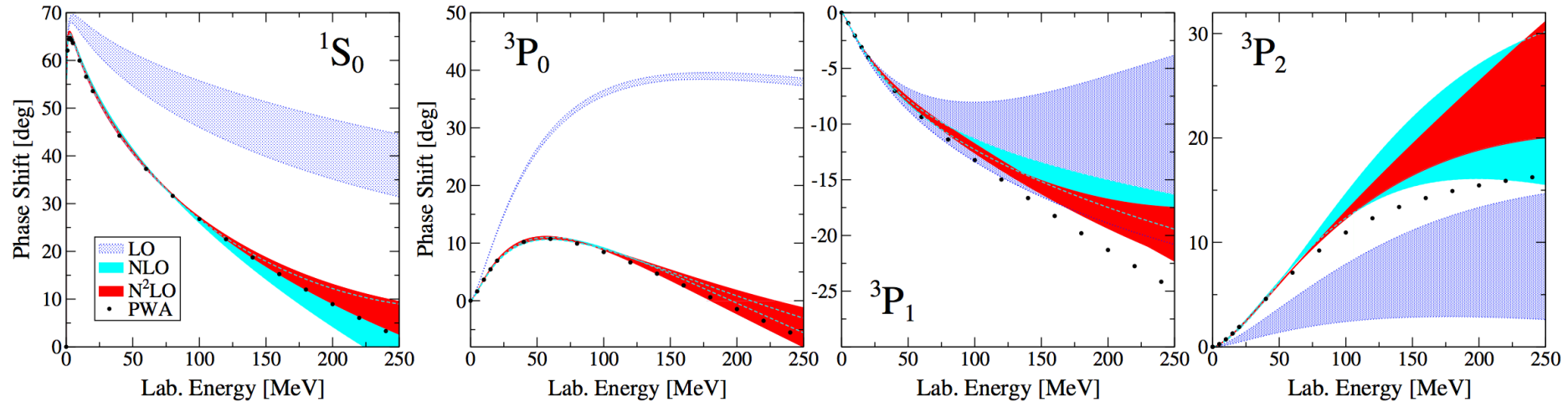
TABLE I. Short-range couplings for $R_0 = 1.2$ fm at LO, NLO, and N²LO (with a spectral-function cutoff $\tilde{\Lambda} = 800$ MeV) [30]. The couplings C_{1-7} are given in fm⁴ while the rest are in fm².

	LO	NLO	N ² LO
C_S	-1.83406	-0.64687	1.09225
C_T	0.15766	0.58128	0.24388
C_1		0.18389	-0.13784
C_2		0.15591	0.07001
C_3		-0.13768	-0.13017
C_4		0.02811	0.02089
C_5		-1.99301	-1.82601
C_6		0.26774	0.18700
C_7		-0.25784	-0.24740
C_{nn}			0.05009

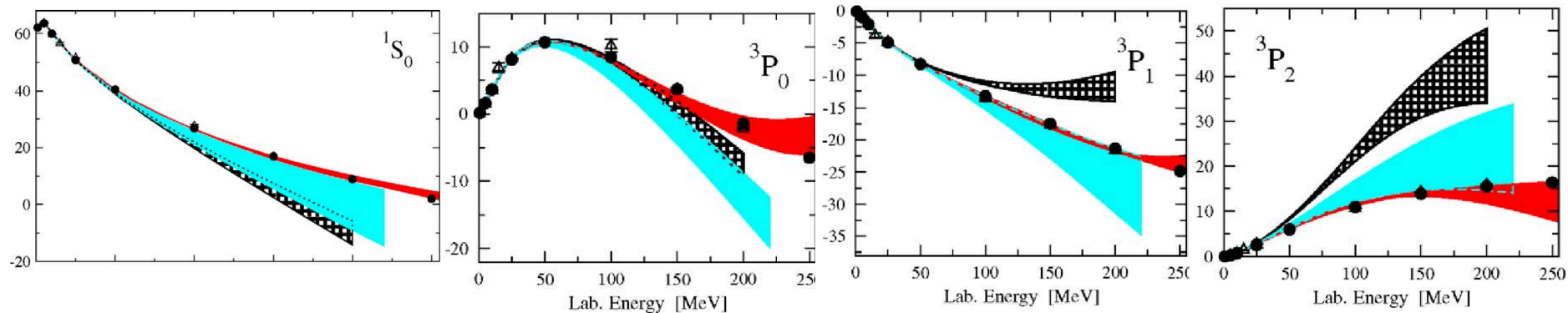
Phase shift fits

fit to $E_{\text{lab}}=1, 5, 10, 25, 50, 100$ MeV, SF cutoff = 800 MeV

vary R_0 from 0.8-1.2 fm, corresponds to ~ 600 -400 MeV



considerably better than EGM N^2 LO potentials



Auxiliary Field Diffusion Monte Carlo

A. Gezerlis, S. Gandolfi

AFDMC: Hubbard-Stratonovich transformation using auxiliary fields to change quadratic spin-isospin operator dependences to linear

include full interaction at LO, NLO, and N²LO in propagator
NN interactions only, next:3N

next: test which parts of chiral EFT interactions are perturbative
(N³LO contributions will have nonlocal parts)

optimal number of 66 particles,
include contributions from 26 neighboring cells of simulation box

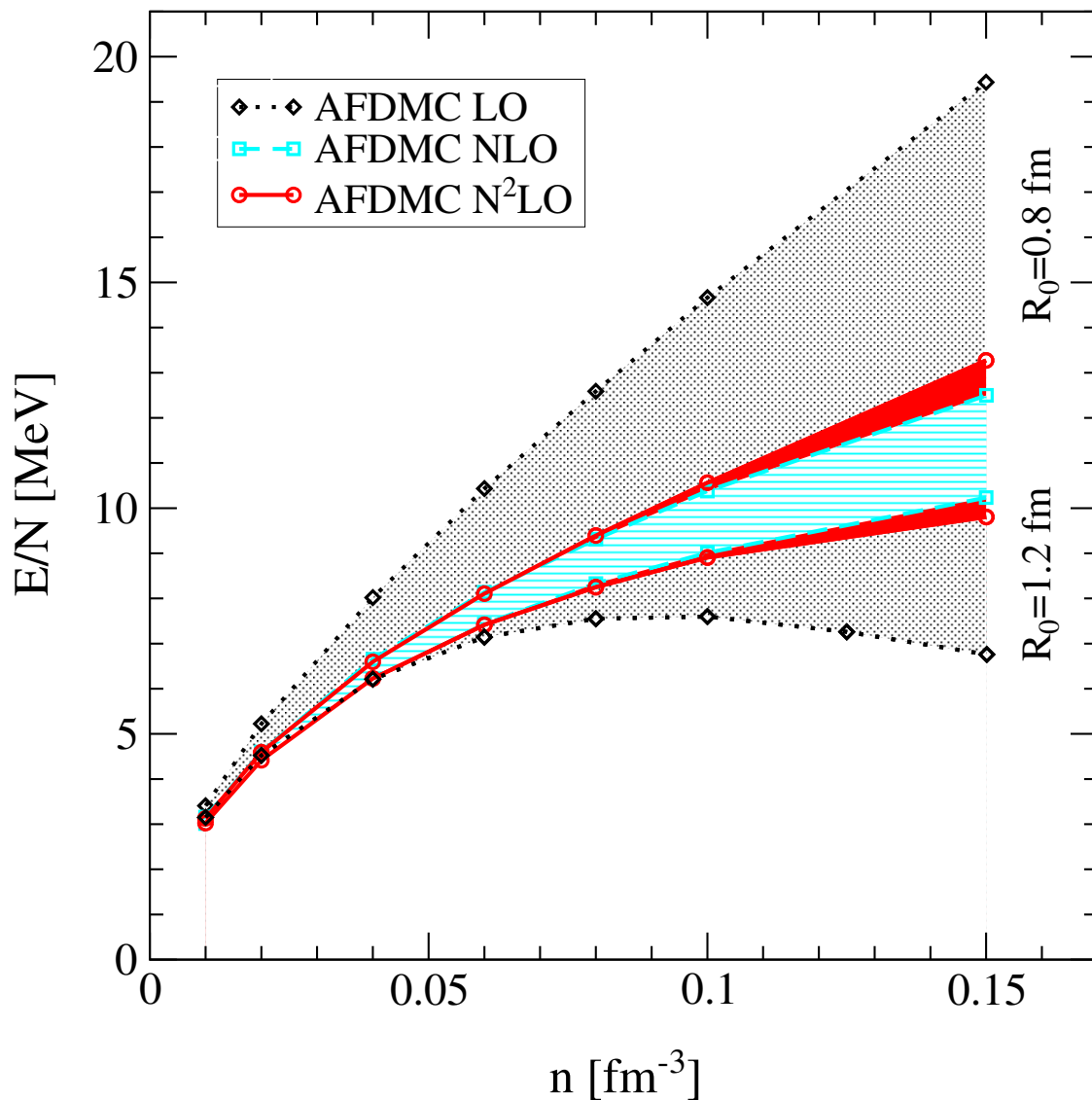
statistical uncertainty smaller than points

no to full Jastrow: 0.1-0.5 MeV (1-5%) for $R_0=1.2-0.8$ fm

AFDMC results for neutron matter

Gezerlis, Tews, Epelbaum, Hebeler, Gandolfi, Nogga, AS, arXiv:1303.63

order-by-order convergence up to saturation density

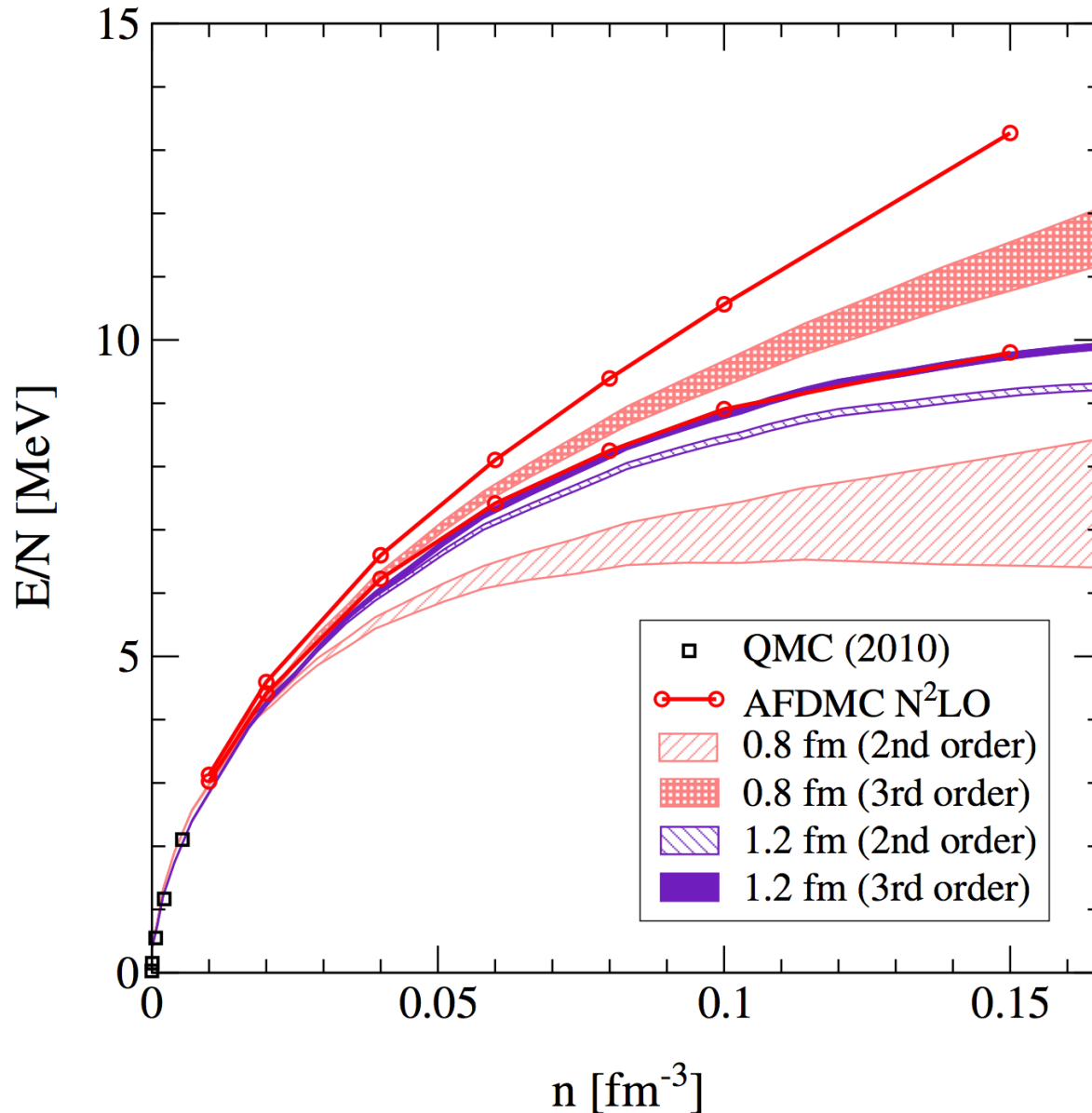


bands similar to
phase shift bands

N^2 LO \sim NLO
due to missing
higher-order contacts

Comparison to perturbative calculations at N²LO

Hartree-Fock +2nd order +3rd order (pp+hh), same as for N³LO calcs.



band at each order from
free to HF spectrum

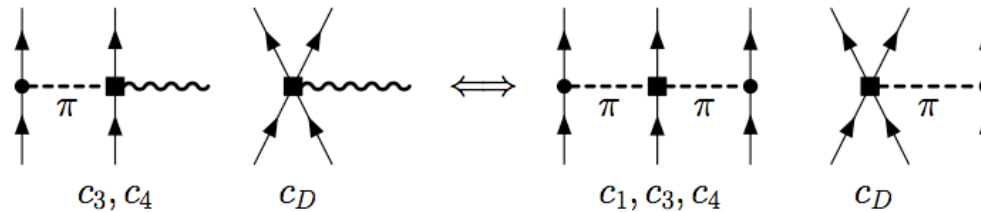
low cutoffs (400 MeV)
3rd order corr. small,
excellent agreement
with AFDMC

Electroweak interactions and 3N forces

weak axial currents couple to spin, similar to pions

two-body currents predicted by NN, 3N couplings to $N^3\text{LO}$

Park et al., Phillips,...



two-body analogue of Goldberger-Treiman relation

explored in light nuclei, but not for larger systems

dominant contribution to Gamow-Teller transitions,
important in nuclei ($Q \sim 100$ MeV)

3N couplings predict quenching of g_A (dominated by long-range part)
and predict momentum dependence (weaker quenching for larger p)

Menendez, Gazit, AS (2011)

Nuclear physics of direct dark matter detection

direct dark matter detection needs **nuclear structure factors** as input, particularly sensitive to nuclear structure for spin-dependent couplings

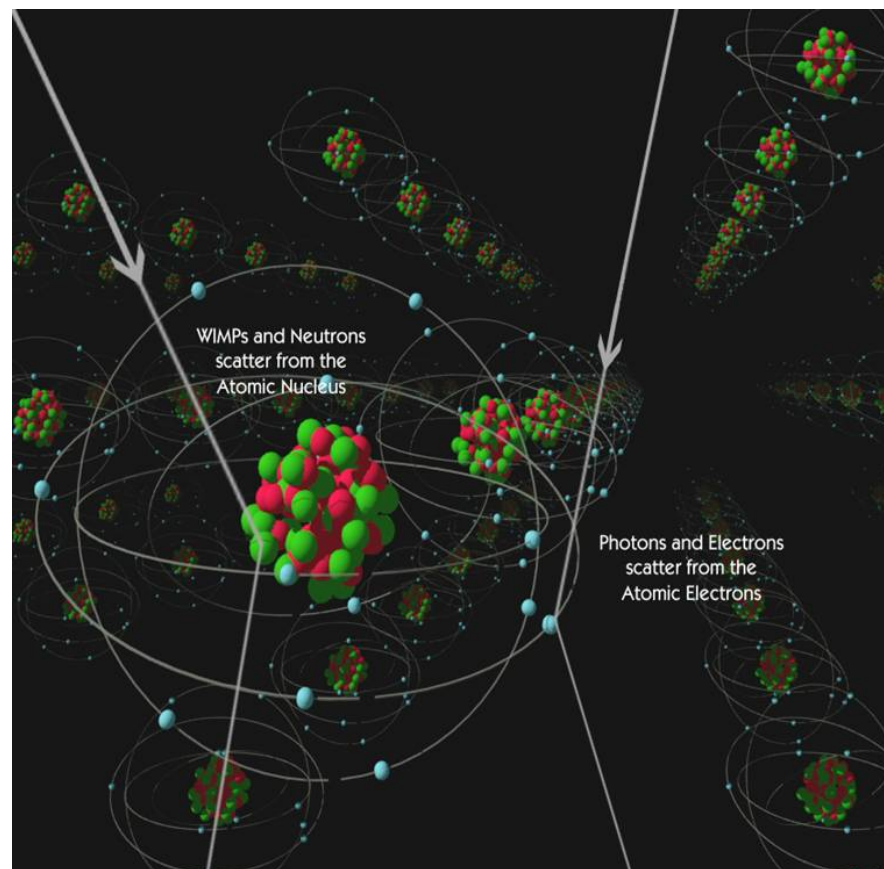
relevant momentum transfers $\sim m_\pi$

**calculate systematically
with chiral EFT**

Menendez et al. (2012)

dark matter response may be complex

Haxton et al. (2012)



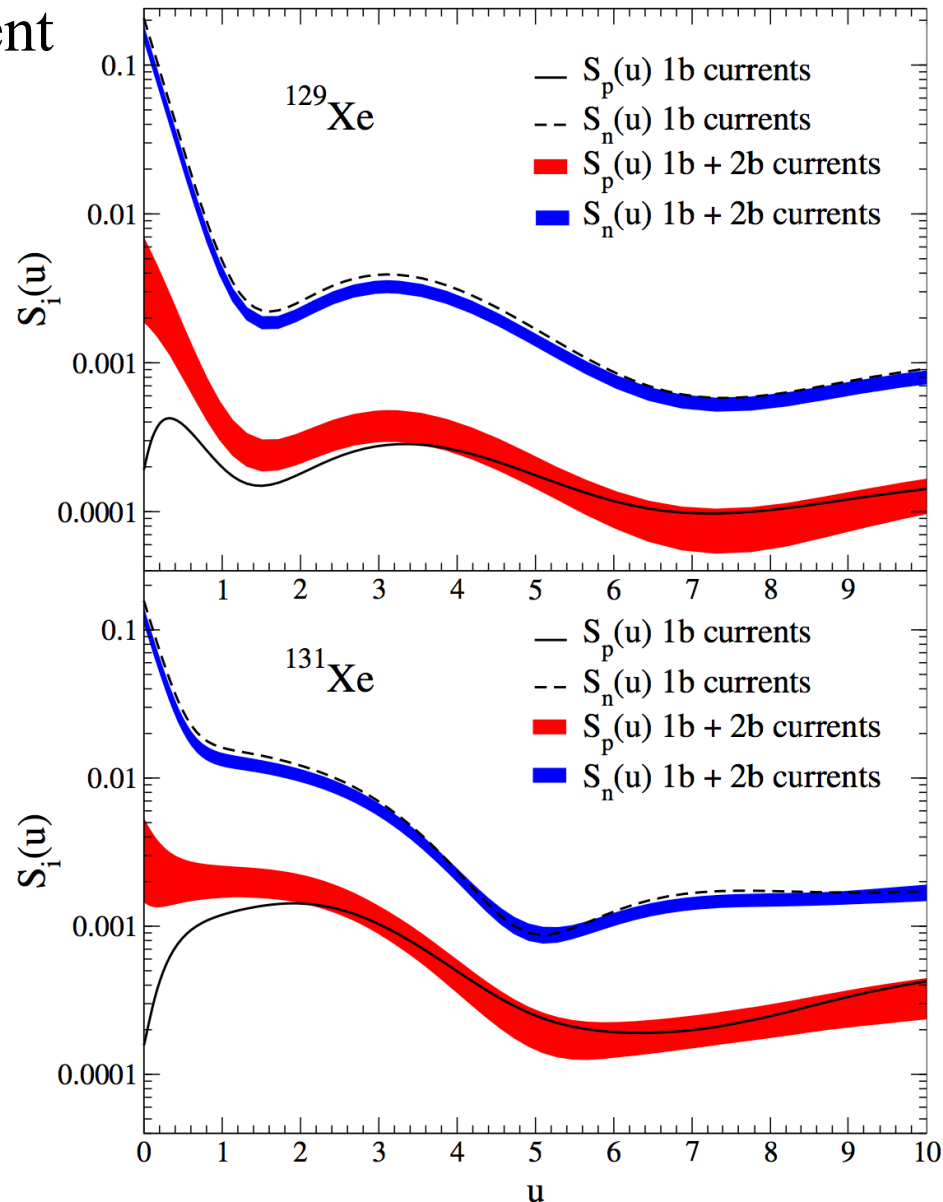
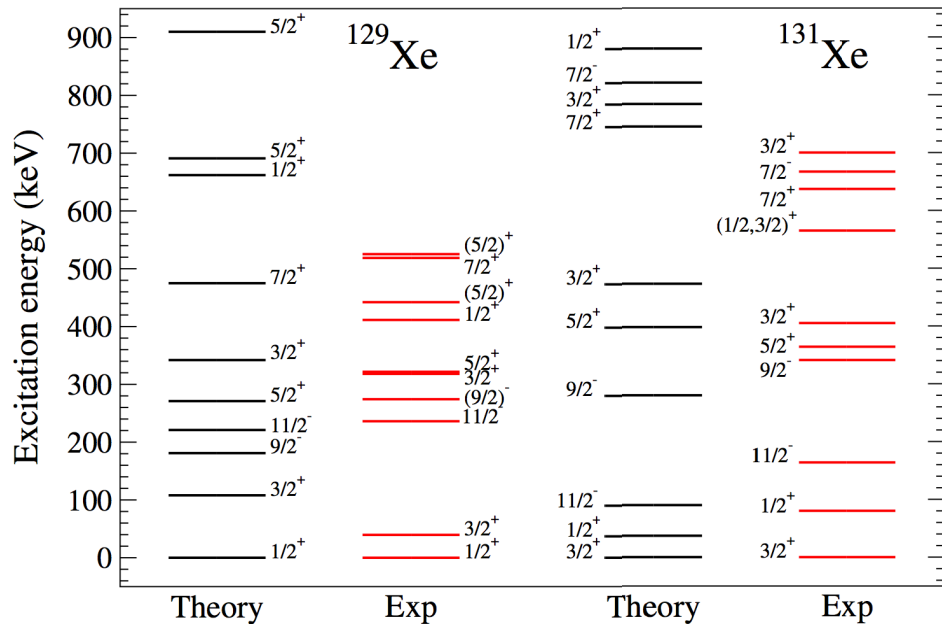
Spin-dependent WIMP scattering off nuclei

spin-dependent WIMP-nucleon interactions
 = isospin rotation of weak axial current

include chiral 2-body currents
 and state-of-the-art interactions

Menendez, Gazit, AS (2012)

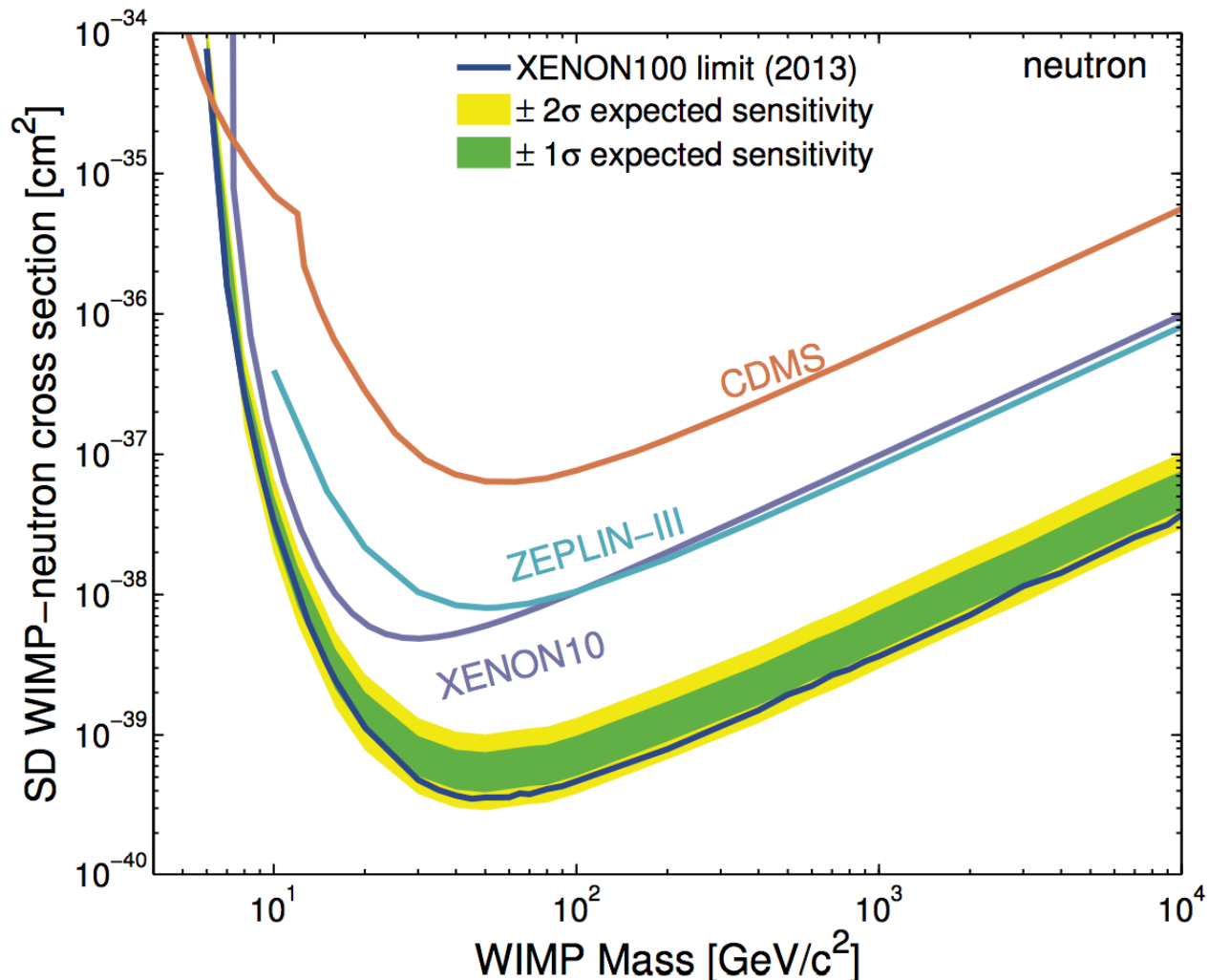
enhances coupling to even-species



Limits on SD WIMP-neutron interactions

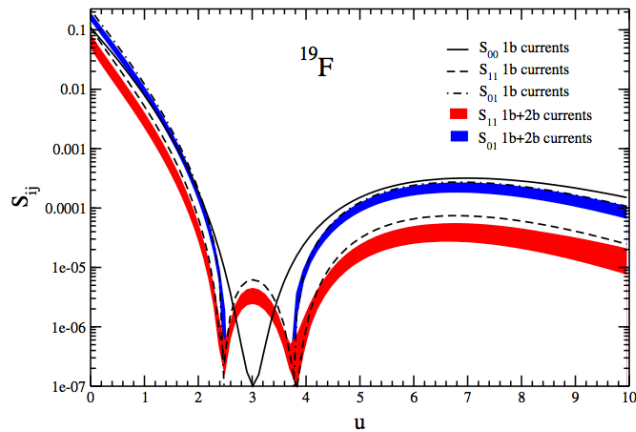
best limits from XENON100 [Aprile et al., 1301.6620](#)

uses Javier Menendez' calculation

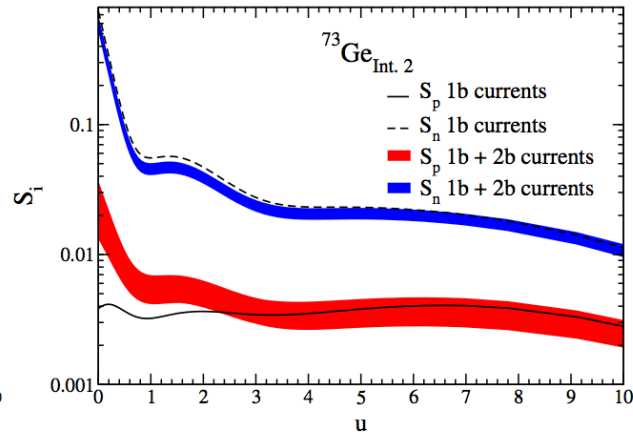


Spin-dependent WIMP-nucleus response for ^{19}F , ^{23}Na , ^{27}Al , ^{29}Si , ^{73}Ge , ^{127}I

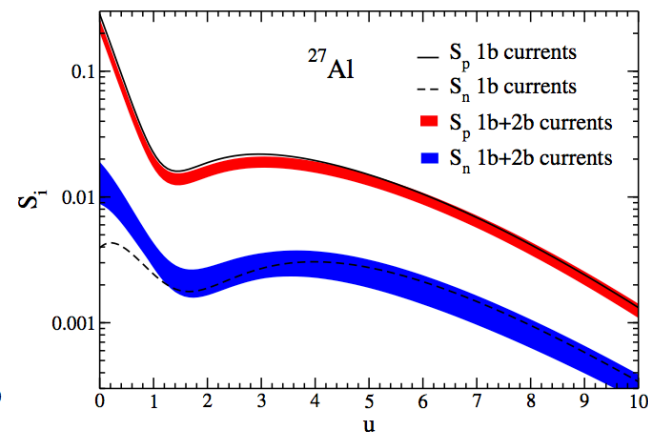
Klos, Menendez, Gazit, AS (2013)



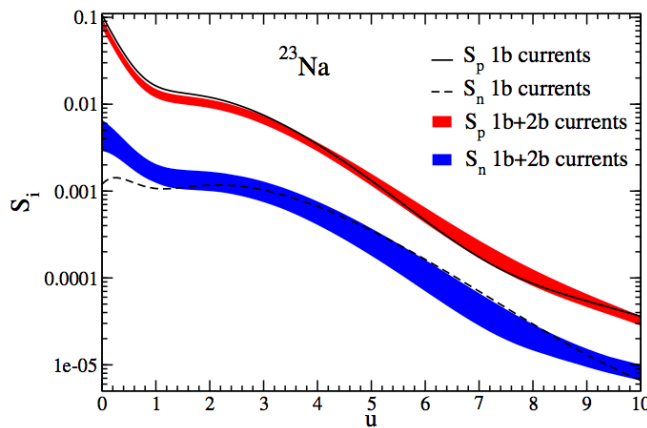
PICASSO, COUPP, SIMPLE



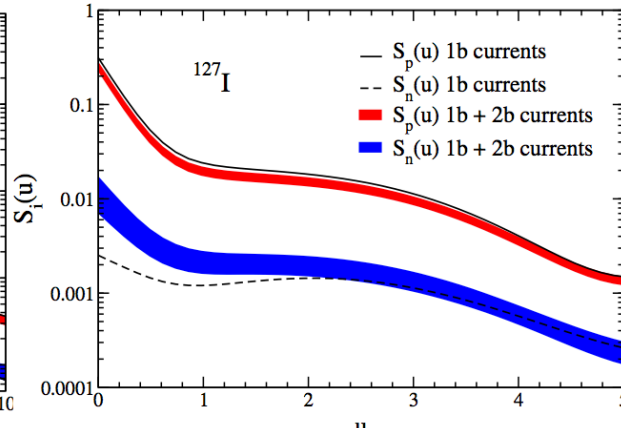
CDMS, EDELWEISS, EURECA



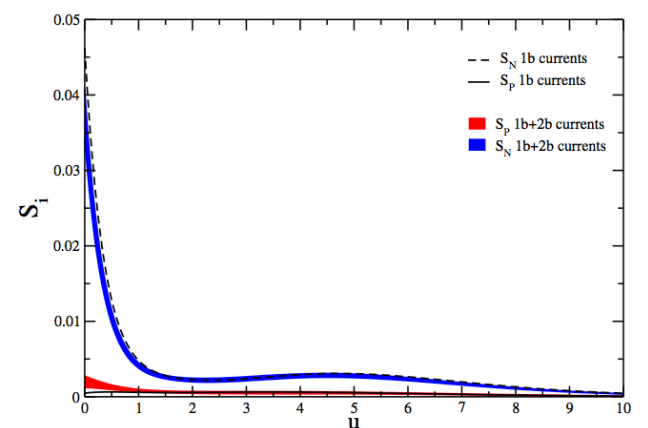
CRESST



DAMA, ANAIS, DM-Ice



DAMA, ANAIS, DM-Ice, KIMS



CDMS-II

Summary

3N forces are a frontier

in chiral EFT, for neutron-rich nuclei, matter, and neutron stars

key for **neutron-rich nuclei**: O, Ca isotopes, N=28 and shell evolution

with J.D. Holt, J. Menendez, T. Otsuka, J. Simonis, T. Suzuki

dominant uncertainty of **neutron (star) matter** below nuclear densities
predicts **neutron skin** with theoretical uncertainty comparable to exp.

constrains **neutron star radii and equation of state** for astrophysics

with K. Hebeler, T. Krüger, I. Tews, J.M. Lattimer, C.J. Pethick

first **QMC calculations with chiral EFT interactions**

with A. Gezerlis, I. Tews, E. Epelbaum, K. Hebeler, S. Gandolfi, A. Nogga

dark matter response of nuclei

with P. Klos, J. Menendez, D. Gazit